Generalized CINE Phase Contrast MRI: High-Pass/Low-Pass Reconstruction

W. S. Kerwin[1], J. Cooke[2], E. Gill[2]

[1]Radiology, University of Washington, Seattle, WA, United States, [2]Cardiology, University of Washington, Seattle, WA, United States

Introduction

CINE phase contrast imaging allows velocity measurements to be made at a sequence of times spanning the cardiac cycle. The result is a sequence of images $I[n]=I_0[n]\exp\{-j(\Phi_0 + \Phi[n])\}$ where n is an index representing the time frame in the cardiac cycle, I_0 and Φ_0 are the baseline magnitude and phase of the image, and $\Phi[n]$ is an induced phase offset proportional to the velocity. Usually, alternating signs of velocity encoding gradients are used in this sequence, which gives $\Phi[n] = \pi \cos(\pi n)\, v[n]/VENC$, where VENC is determined by the velocity encoding gradient. Velocities are then computed based on the phase difference between successive images in the sequence, where phase difference is used to eliminate the unknown Φ_0 and is the motivation for alternating the sign of the encoding gradient. Although effective, this approach for measuring velocities sometimes suffers from long scan times due to the need for two sets of images and can have high noise due to the sensitivity of phase to random noise. To permit flexibility in determining scan time, SNR, and temporal resolution, a new high-pass/low-pass (HPLP) filtering formulation is proposed here for reconstructing CINE phase contrast data and used to develop an UNFOLD [1] based technique for rapid imaging of velocities.

Theory and Methods

If I[n] above is expanded using Euler's equation, the image sequence can alternatively be written $I[n]=L[n] - j\cos(\pi n)\, H[n]$, where $L[n] = I_0[n]\exp\{-j\Phi_0\}\cos(\pi\, v[n]/VENC)$ and $H[n] = I_0[n]\exp\{-j\Phi_0\}\sin(\pi\, v[n]/VENC)$. The ratio of these two components is $H[n]/L[n] = \tan(\pi\, v[n]/VENC)$, from which velocity can be directly extracted regardless of I_0 and Φ_0. Therefore, this ratio provides an alternative technique for computing velocity *if* H[n] and L[n] can be separated. Fortunately, in the equation for I[n], H[n] is modulated by $\cos(\pi n)$, which shifts it to high frequency regions. H[n] and L[n] can then be separated by high and low pass filtering, respectively.

In fact, this is in a sense what happens when the traditional phase difference method is used. The tangent of the phase difference between I[n] and I[n+1] is equal to the imaginary part of $\{(I[n+1]-I[n])/(I[n+1]+I[n])\}$. The numerator of this equation is a high-pass filter and the denominator is a low-pass filter, which makes the traditional reconstruction approach a form of HPLP reconstruction. Because HPLP reconstructed is not limited to these filters, it generalizes phase contrast MRI. One benefit of HPLP reconstruction occurs if the bandwidths of H[n], L[n], and the filters are all narrow. In this case, most of the noise (which spreads throughout the spectrum) will be eliminated from the velocity measurements by the filters. Moreover, regions where narrow band filters are sufficient enable the principles of UNFOLD [1,2] to be applied to undersample k-space and map the aliased signals into the unused midrange frequencies. Because these midrange frequencies are eliminated by the high-pass and low-pass filters, the true velocity can be extracted despite the undersampling of k-space. The benefit of this approach is an acquisition time savings.

To test these theories, sequences for CINE phase contrast MRI with UNFOLD were designed that mapped aliased image components to midrange frequencies and had acceleration factors of 2 and 4. Human volunteers and a simple tube phantom driven by a cardiac pump were imaged. All were run on a 1.5T scanner (GE Medical Systems, WI) within a gradient echo phase contrast acquisition with a repetition time of 14 msec. When scanning human volunteers, axial image slices were used with a 32x16 cm FOV and 128x64 matrix leading to 2.5 mm in-plane resolution. A 4X UNFOLD acceleration was used, which led to a total breath-held scan time of 16 heartbeats.

Figure 1

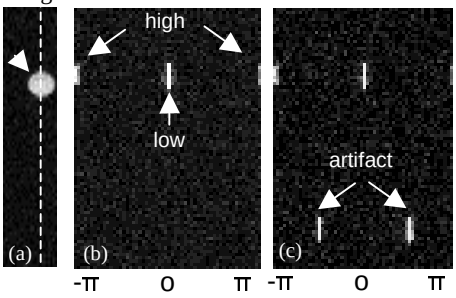

Results

The presence of low and high frequency components in the CINE phase contrast image sequence is illustrated in Figure 1 for the tube phantom. Figure 1a shows a section of a magnitude image with the tube in cross section. Figure 1b shows the frequency distribution of each pixel along the indicated line in 1a. The existence of separate high and low frequency components H[n] and L[n] is evident. Figure 1c shows the effect of the UNFOLD acquisition on this picture in which artifactual components appear at midrange frequencies. The low and high pass filters reject these midrange frequencies allowing the true velocity to be computed as illustrated in Figure 2. This figure compares the velocity versus time at the center of the tube, computed using the traditional phase difference approach (solid line) to those obtained with HPLP reconstruction in ½ the time with 2X UNFOLD (dashed) and in ¼ the time with 4X UNFOLD (dash-dot). Finally, Figure 3 shows the ability of this technique to map the flow field in the human left ventricle. In this early diastolic image of the long axis of the left ventricle, a vortex (arrow) is evident near the tip of the anterior mitral valve leaflet.

Conclusions

This study validates the theory behind the new HPLP reconstruction technique. Phantom experiments show that CINE phase contrast MRI leads to separate high and low temporal frequency components, and that UNFOLD can be used to map aliased signals to the midrange frequencies between these components. HPLP reconstruction then accurately recovers the same velocity tracings as traditional phase contrast MRI, but in much less time. Applied to the human heart, this technique was shown to be robust enough to capture the vortex that appears during inflow, as previously reported [3]. This fast imaging technique could also be combined in principle with other accelerated approaches for phase contrast imaging (e.g. [4]) for ultrafast imaging.

Figure 2

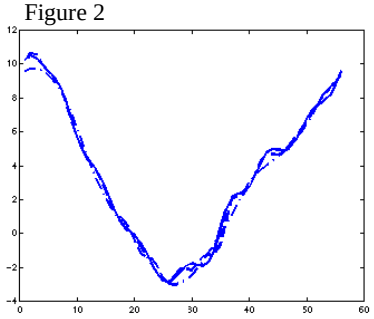

Figure 3

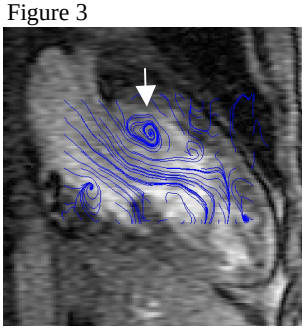

References

1. Madore et al. *MRM* 42:813-828, 1999.
2. Tsao *MRM* 47:202-207, 2002.
3. Kim et al. *JACC* 26:224-238, 1995.
4. Markl & Hennig *MRI* 19:669-676, 2001.